Electronic Supplementary Information

Ratiometric chemodosimeter: an organic-nanofiber platform for sensing lethal phosgene gas

Kalipada Maiti,[a] Debasish Ghosh,[a] Rituparna Maiti,[a] Vena Vyas,[b] Pallab Datta,[b] Debabrata Mandal*[a] and Dilip K Maiti*[a]

[a] Department of Chemistry, University of Calcutta, University College of Science, 92, A. P. C. Road, Kolkata 700009, India. [b]Department of Health Care Science, Indian Institute of Engineering Science and Technology, Shibpur, Howrah 711103, India.

Table of Contents

1. General information

All reagents were purchased from commercial suppliers and used without further purification. Petroleum ether used in our experiments was in the boiling range of 60-80 °C. Column chromatography was performed on silica gel (100-200 mesh and 230-400 mesh). Reported melting points are uncorrected. ^{1}H NMR and ^{13}C NMR spectra were recorded at ambient temperature in $CDCl_3$/DMSO-d_6 solution. Chemical shift are reported in ppm (δ) relative to internal reference tetramethylsilane. Coupling constants are quoted in Hz (J). Proton multiplicities are represented as s (singlet), d (doublet), dd (doublet of doublet), t (triplet), q (quartet), and m (multiplet). Splitting patterns that could not be interpreted were designated as multiplet (m). HR-MS data were acquired by electron spray ionization technique on a Qtof micro quadriple mass spectrophotometer.

2. Characterization data of the synthesized compounds

Compound 2 to 4 has been synthesized by following procedure of the previously reported literature.[1]

2.1. 4-Bromo-*N*-butyl-1,8-naphthalimide (2)[1]

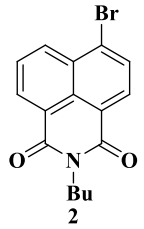

2

White solid; yield: 90%; ^{1}H NMR (300 MHz, $CDCl_3$): δ 8.67 (dd, J_1 = 7.3 Hz, J_2 = 1.2 Hz, 1H), 8.58 (dd, J_1 = 8.4 Hz, J_2 = 1.2 Hz, 1H), 8.42 (d, J = 8.1 Hz, 1H), 8.05 (d, J = 7.8 Hz, 1H), 7.89-7.83 (m, 1H), 4.18 (t, J = 7.8 Hz, 2H), 1.75-1.68 (m, 2H), 1.46 (q, J = 7.5 Hz, 2H), 0.99 (t, J = 7.5 Hz, 3H).

2.2. 4-Methoxy-*N*-butyl-1,8-naphthalimide (3)[1]

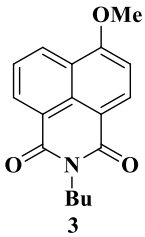

3

Pale yellow solid; yield: 80%, ^{1}H NMR (300 MHz, $CDCl_3$): δ 8.57-8.50 (m, 3H), 7.67 (t, *J* = 7.5 Hz, 1H), 7.01 (d, *J* = 8.4 Hz, 1H), 4.19-4.12 (m, 5H), 1.74-1.68 (m, 2H), 1.49-1.41 (m, 2H), 0.98 (t, *J* = 7.5 Hz, 3H), ; ^{13}C NMR (75 MHz, $CDCl_3$): δ 164.4, 163.9, 160.7, 133.3, 131.4, 129.3, 128.4, 125.8, 123.4, 122.4, 115.1, 105.1, 56.1, 40.0, 30.2, 20.3, 13.8.

2.3. 4-Hydroxy-*N*-butyl-1,8-naphthalimide (4)[1]

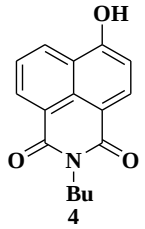

4

Yellow solid; yield: 60%; ^{1}H NMR (300 MHz, $CDCl_3$): δ 12.52 (s, 1H), 8.92 (d, *J* = 8.4 Hz, 1H), 8.86 (d, *J* = 7.2 Hz, 1H), 8.75 (d, *J* = 8.1 Hz, 1H), 8.15 (t, *J* = 7.8 Hz, 1H), 7.55 (dd, J_1 = 8.1 Hz, J_2 = 2.4 Hz, 1H), 4.41 (t, *J* = 7.5 Hz, 2H), 1.99 (t, *J* = 7.2 Hz, 2H), 1.76-1.70 (m, 2H), 1.35-1.31 (m, 3H).

2.4. 3-fromyl 4-Hydroxy-*N*-butyl-1,8-naphthalimide (5)[1]

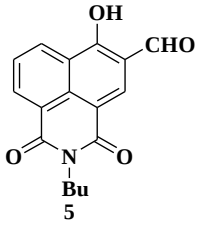

5

Yellow solid; yield: 85%; ^{1}H NMR (300 MHz, $CDCl_3$): δ 13.20 (s, 1H), 10.13 (s, 1H), 8.74 (t, *J* = 8.4 Hz, 3H), 7.83 (t, *J* = 8.1 Hz, 1H), 4.19 (t, *J* = 6.8 Hz, 2H), 1.67-1.75 (m, 2H), 1.30-1.47 (m, 2H), 1.02-1.30 (m, 3H).

2.5. (*E*)-2-butyl-6-hydroxy-1,3-dioxo-2,3-dihydro-1*H*-benzo[*de*]isoquinoline-5-carbaldehyde oxime (R1)

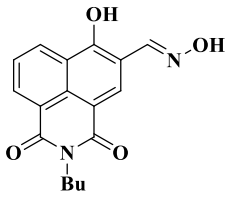

Compound **5** (250 mg, 0.84 mmol) was dissolved in dry ethanol (15 ml). Then triethylamine (0.18 ml, 1.5 equiv.) and hydroxylamine hydrochloride (60 mg, 0.86 mmol) were added. The resulting mixture was

refluxed for 4 hrs. A yellow precipitate was arisen. Then the precipitate was washed with water thoroughly. The crude was then recrystallized in $CHCl_3$-MeOH (1:1) mixture. Yellow solid; yield: 72% (188 mg);; ^{1}H NMR (300 MHz, DMSO-d^6): δ 11.88 (brs, 1H), 8.69 (s, 1H), 8.56-8.52 (m, 2H), 8.43 (d, *J* = 6.9 Hz, 1H), 7.77 (t, *J* = 7.8 Hz, 1H), 5.77 (s, 1H), 3.99 (t, *J* = 7.5 Hz, 2H), 1.63-1.53 (m, 2H), 1.39-1.27 (m, 2H), 0.91 (t, *J* = 7.2 Hz, 3H), ; ^{13}C NMR (75 MHz, $CDCl_3$): δ 162.9, 162.2, 158.2, 148.9, 131.8, 131.0, 128.5, 128.0, 125.9, 122.0, 121.4, 112.9, 112.8, 39.8, 29.2, 19.3, 13.2; HR-MS (*m*/*z*) for $C_{17}H_{17}N_2O_4$ (M+H) : Calculated 313.1110, found 313.1112 (M^++H).

3. Determination of concentration of Et_3N required for conversion of triphosgene to phosgene

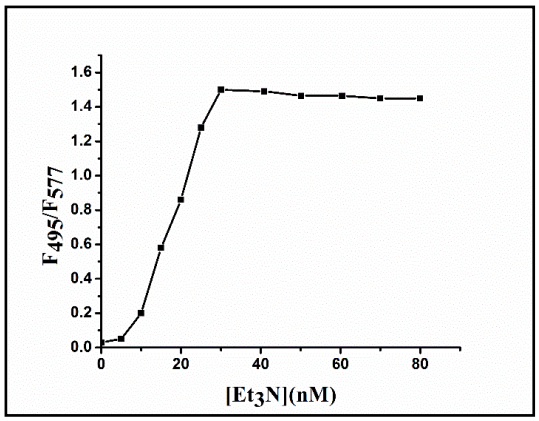

Figure S1: Change in Fluorescence intensity ratio (F_{495}/F_{577}) of the solution sample containing **R1** (10 μM) and triphosgene (0.5 equiv.) as a function of the concentration of Et_3N.

4. Plot of Fl. Intensity ratio vs concentration of triphosgene

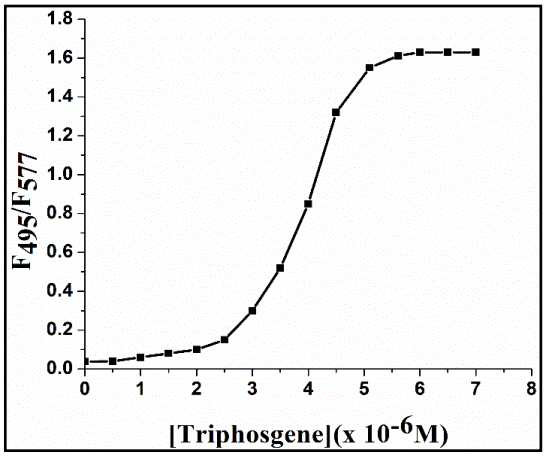

Figure S2: Change in Fluorescence intensity ratio (F_{495}/F_{577}) of the solution sample containing **R1** (10 μM) and Et_3N (0.5%) as a function of the concentration of triphosgene.

5. Calculation of detection limit and photo stability of the probe R1

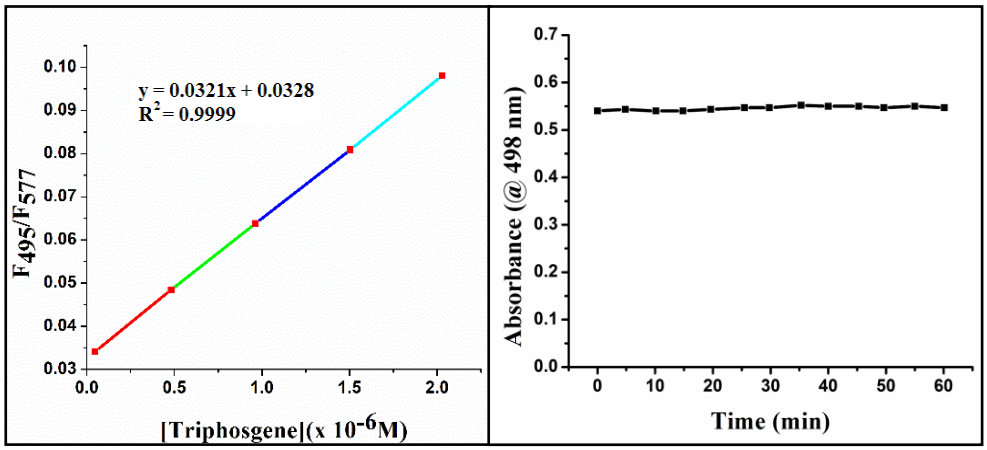

Figure S3: Linearship of fluorescence intensity ratio (F_{495}/F_{445}) of **R1** (10 μM) to triphosgneconcentration (0-2.0 μM) in the presence of triethylamine (30 nM, 0.5%). (b) Time variation of **R1**absorption peak at 498 nm after UV irradiation. Similar results were observed for **R1**/PCL nanofiber, **R1**/PCL film and R1-embeded filter paper.

6. Time dependent fluorescence spectra of R1/filter paper, R1/PCL film and R1/PCL nano fiber

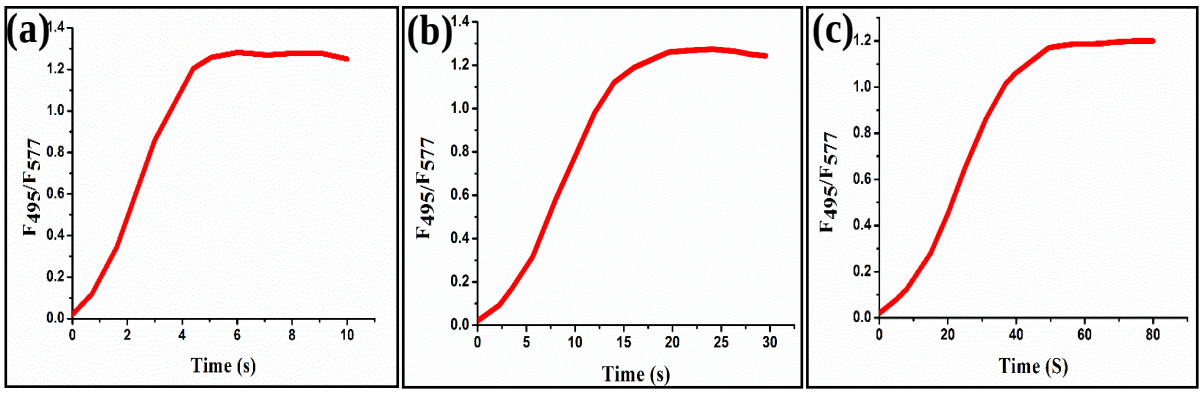

Figure S4: Time dependent fluorescence spectra of (a) **R1**/PCL nano fiber, (b)**R1**/PCL and (c)**R1**/filter paper in presence of phosgene (0.5 ppm).

7. Fluorescence spectra of R1 in presence of formaldehyde and NO

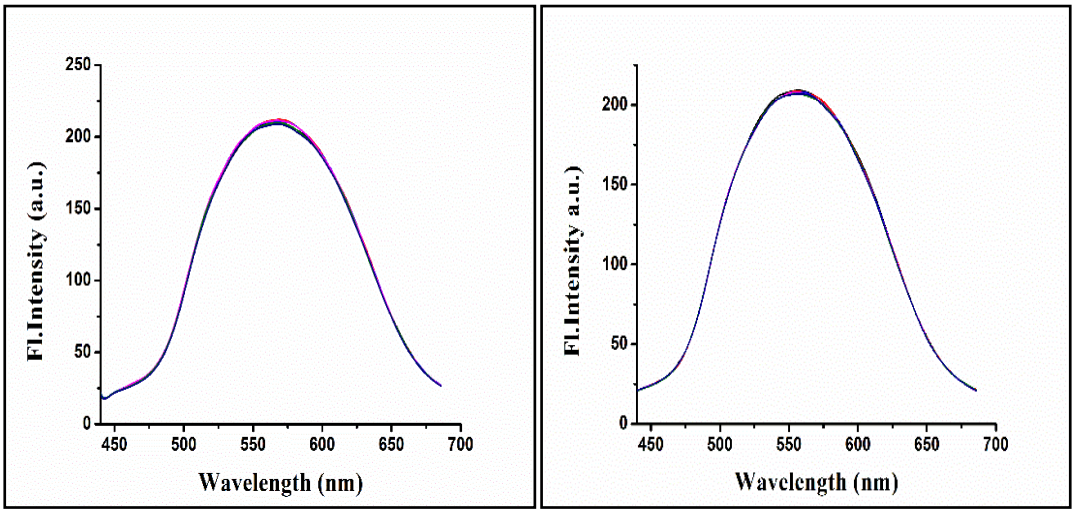

Figure S5: Fluorescence spectra of 10 μM probe **R1** in AcCN, upon gradual addition of (a) formaldehyde (5 equiv.) and (b) NO (5 equiv.).

8. LOD (Limit of detection) of phosgene in R1/filter paper, R1/PCL film and R1/PCL nano fiber

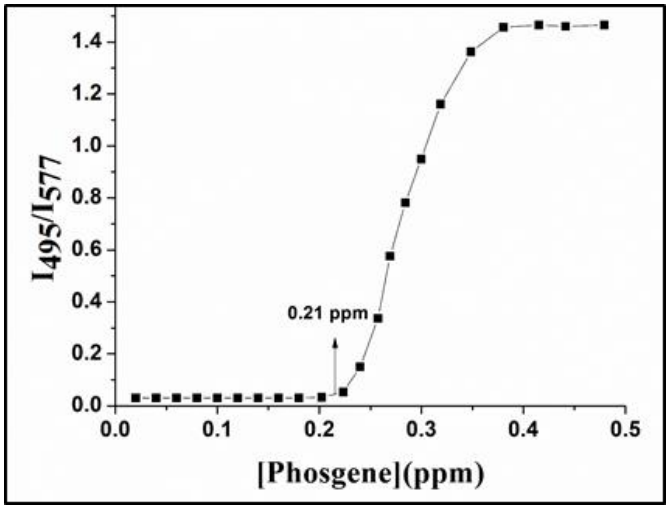

Figure S6: Change in Fluorescence intensity ratio (F_{495}/F_{577}) of the filter paper immersed with sample containing **R1** (1.0 mg/1 ml AcCN) and Et_3N (0.5%) as a function of the concentration of triphosgene.

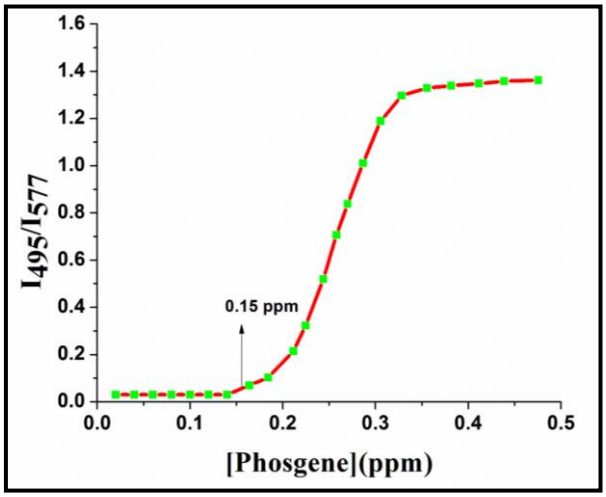

Figure S7: Change in Fluorescence intensity ratio (F_{495}/F_{577}) of the PCL/**R1** film and Et_3N (0.5%) as a function of the concentration of triphosgene.

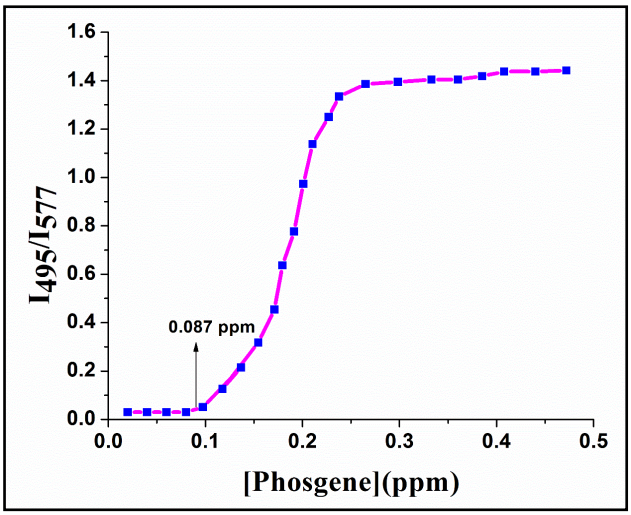

Figure S8: Change in Fluorescence intensity ratio (F_{495}/F_{577}) of the PCL/**R1** nano fiber and Et_3N (0.5%) as a function of the concentration of triphosgene.

9. Kinetics study

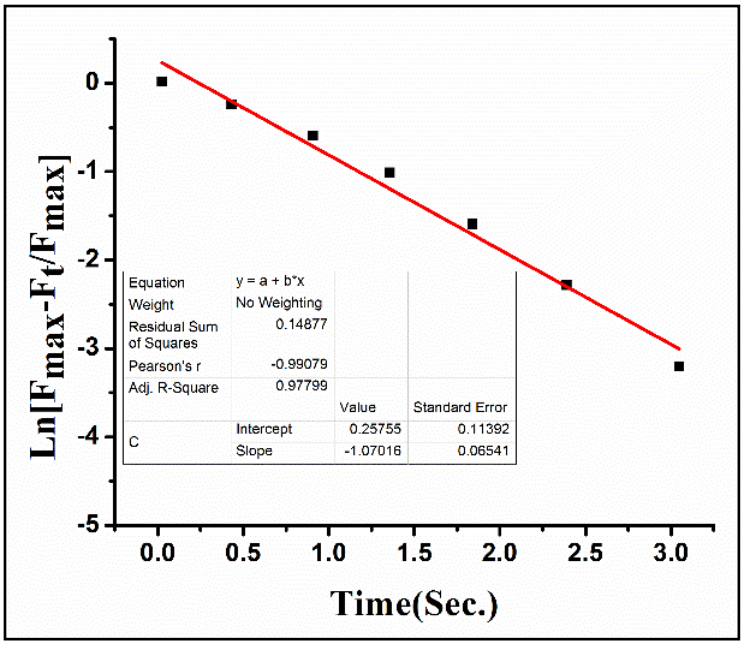

Figure S9: Graph of Pseudo first order rate of **R1** (10 μM) in AcCN in presence of triphosgene (5 equiv.). [Rate constant ($k^{/}$ = 1.07016 s^{-1})].

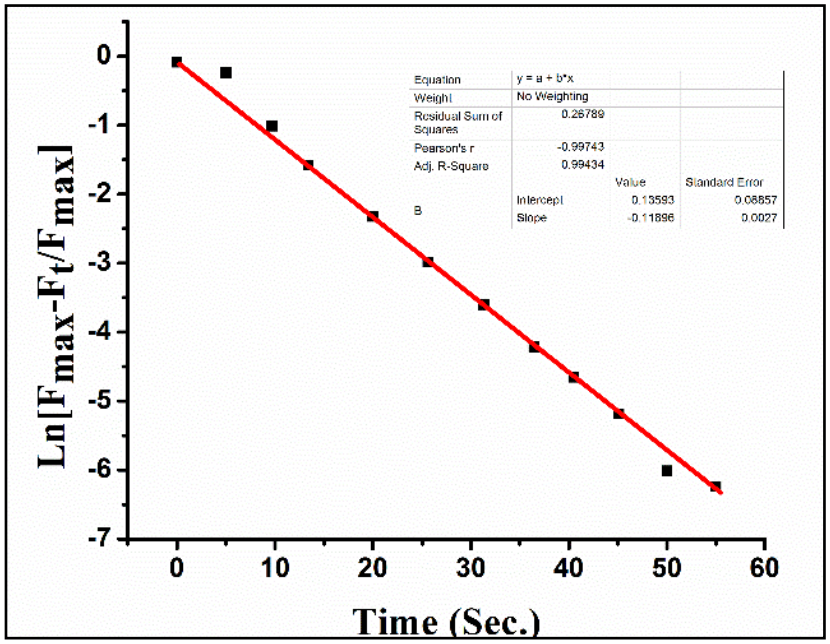

Figure S10: Graph of Pseudo first order rate of **R1**/ filter paper in presence of triphosgene (0.5 ppm). [Rate constant ($k^{/}$ = 0.11896 s^{-1})].

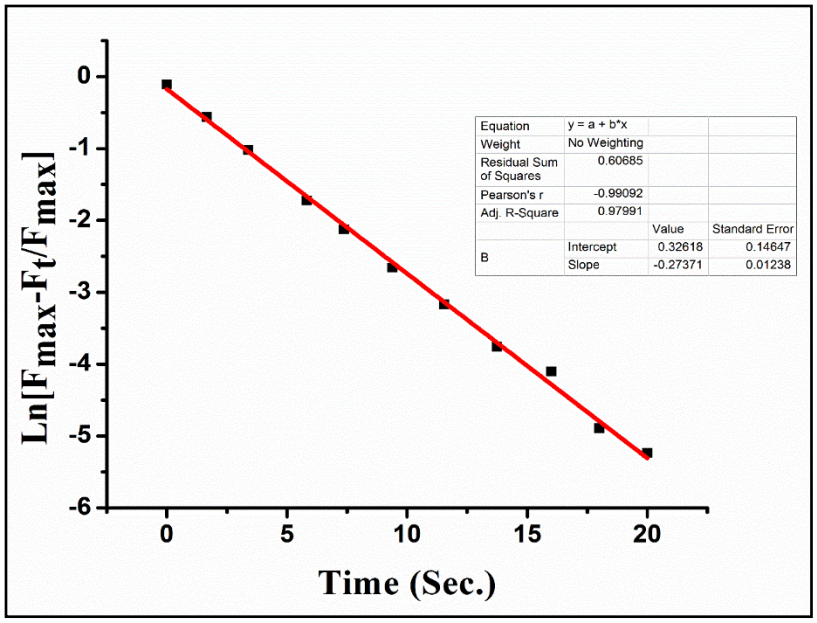

Figure S11: Graph of Pseudo first order rate of **R1**/ PCL film in presence of triphosgene (0. 5 ppm). [Rate constant ($k^{/}$ = 0.27371 s^{-1})].

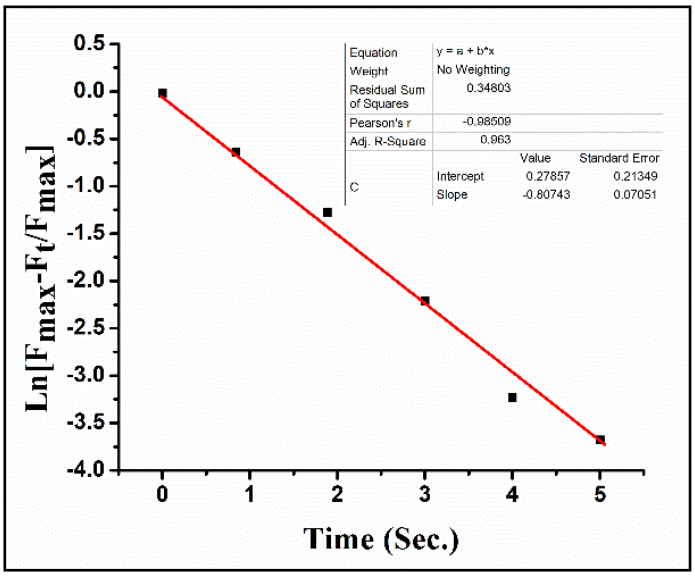

Figure S12: Graph of Pseudo first order rate of **R1**/PCL nano fiber in presence of triphosgene (0.5 ppm). [Rate constant ($k^{/}$ = 0.80743 s^{-1})].

10. Table S1: LOD, response time and rate constant of different protocol towards phosgene

Solid protocol	LOD (/min)	Response time (S)	Rate constant (S^{-1})
Filter Paper	0.21 ppm	45	0.118
R1/PCL film	0.15 ppm	20	0.27
R1/PCL nano fiber	0.087 ppm	< 5	0.807

11. Different spectra for characterization of synthesized compounds

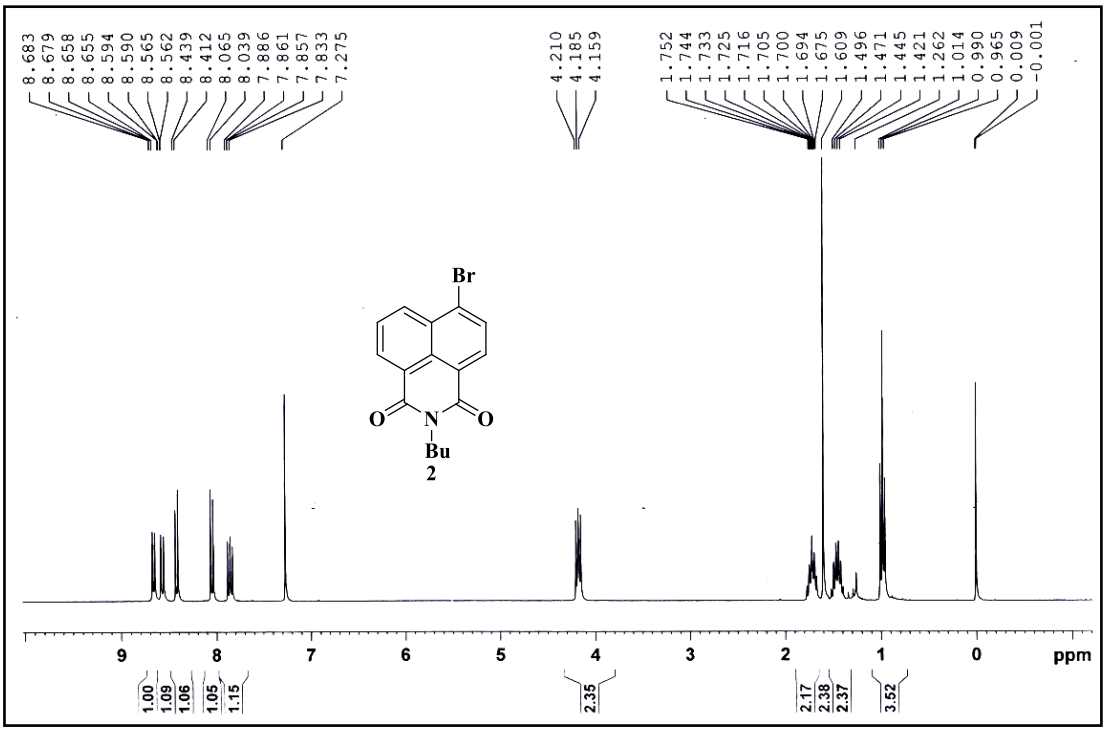

Figure S13: ^{1}H NMR of Compound **2**

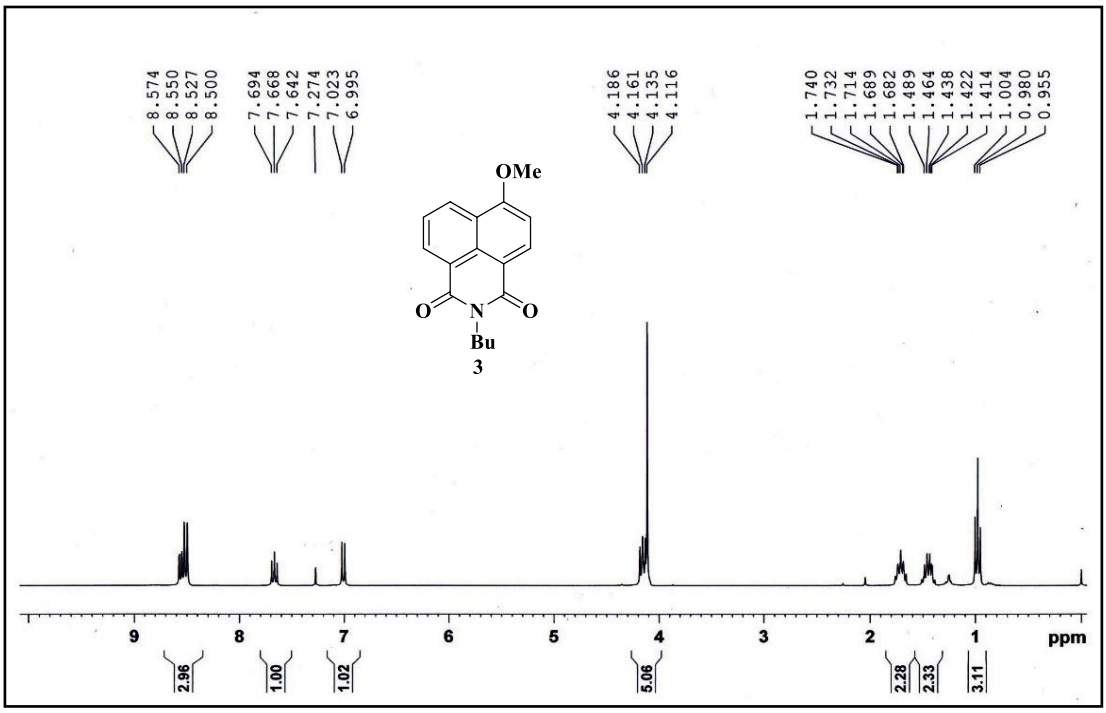

Figure S14: ^{1}H NMR of Compound **3**

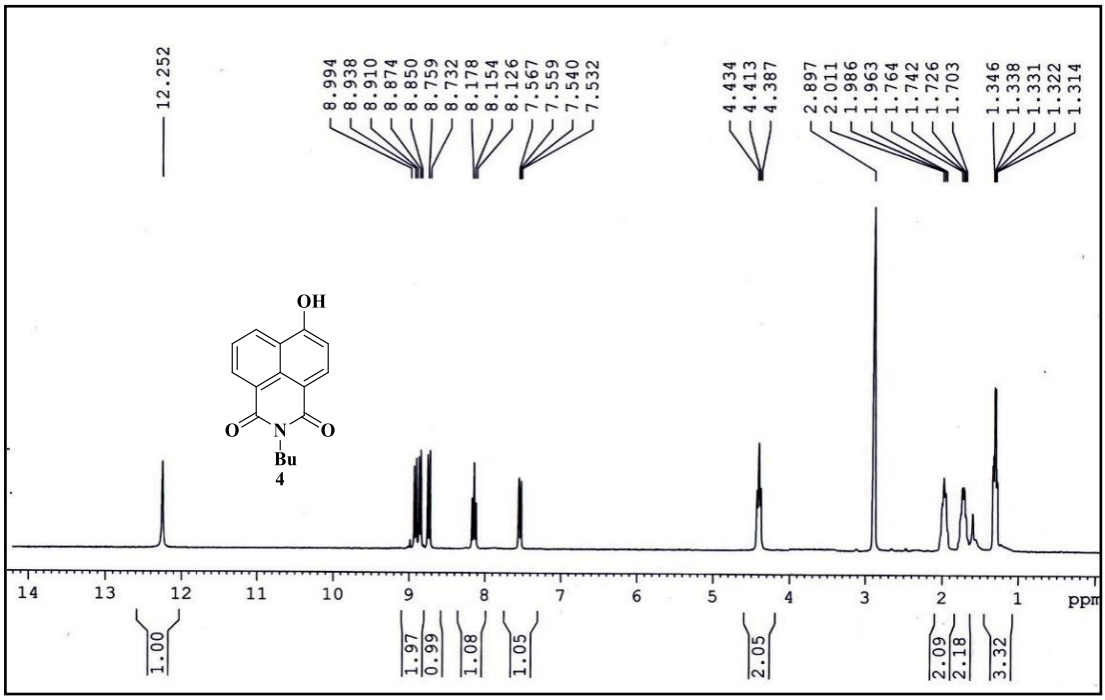

Figure S15: ^{1}H NMR of Compound **4**

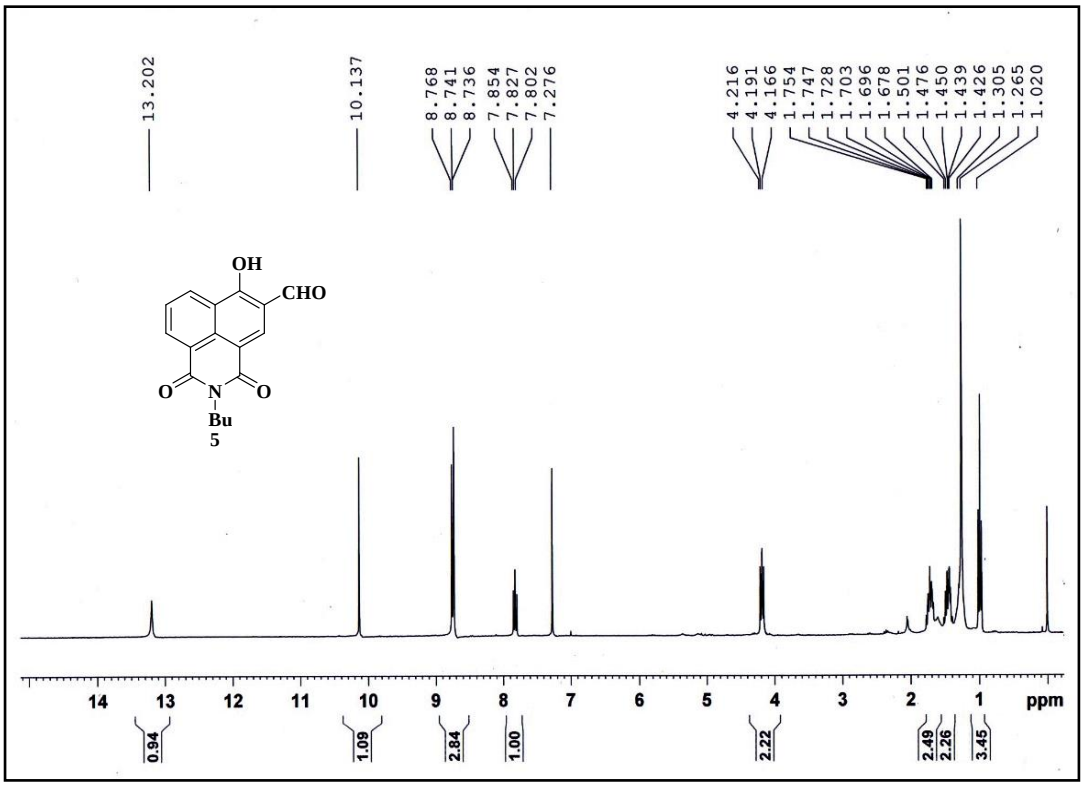

Figure S16: ^{1}H NMR of Compound **5**

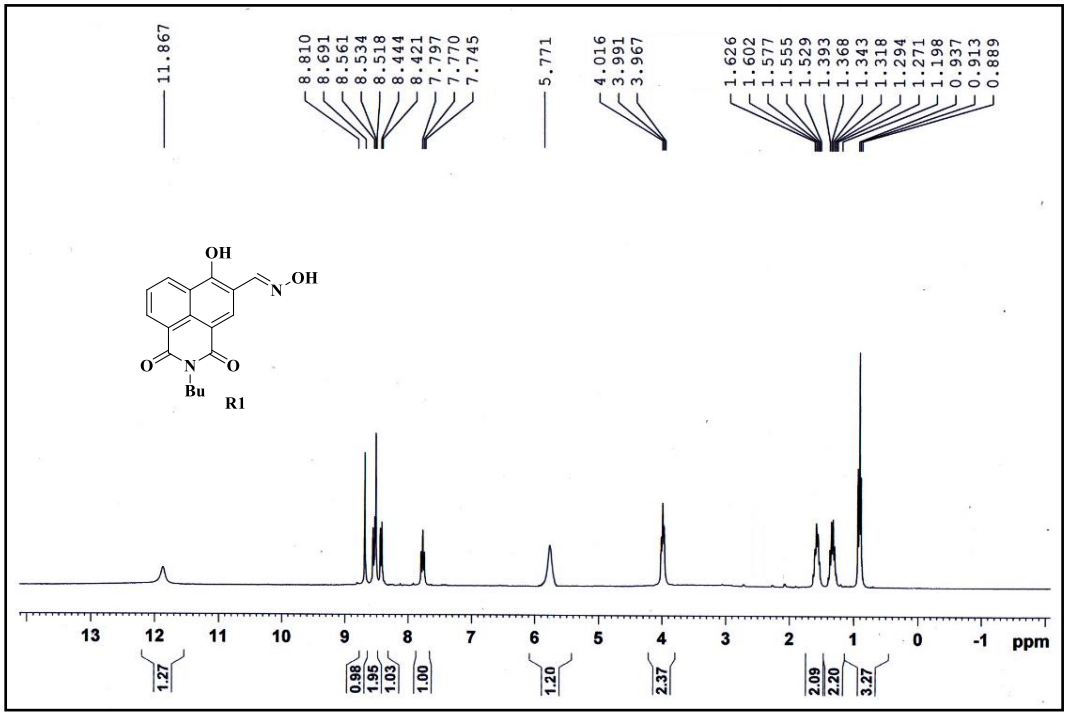

Figure S17: ^{1}H NMR of Compound **R1**

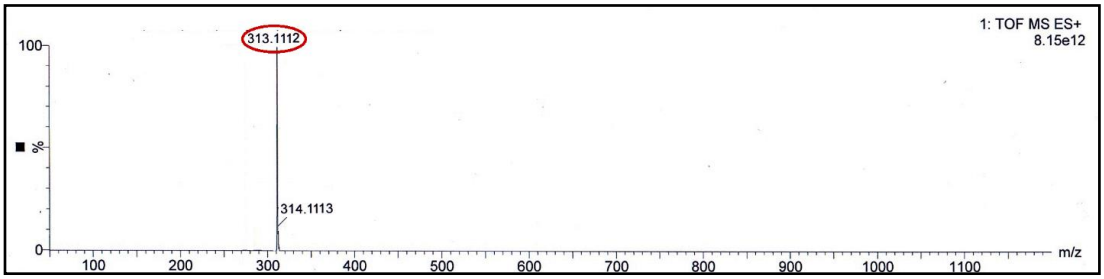

Figure S18: ESI-MS of Compound **R1**

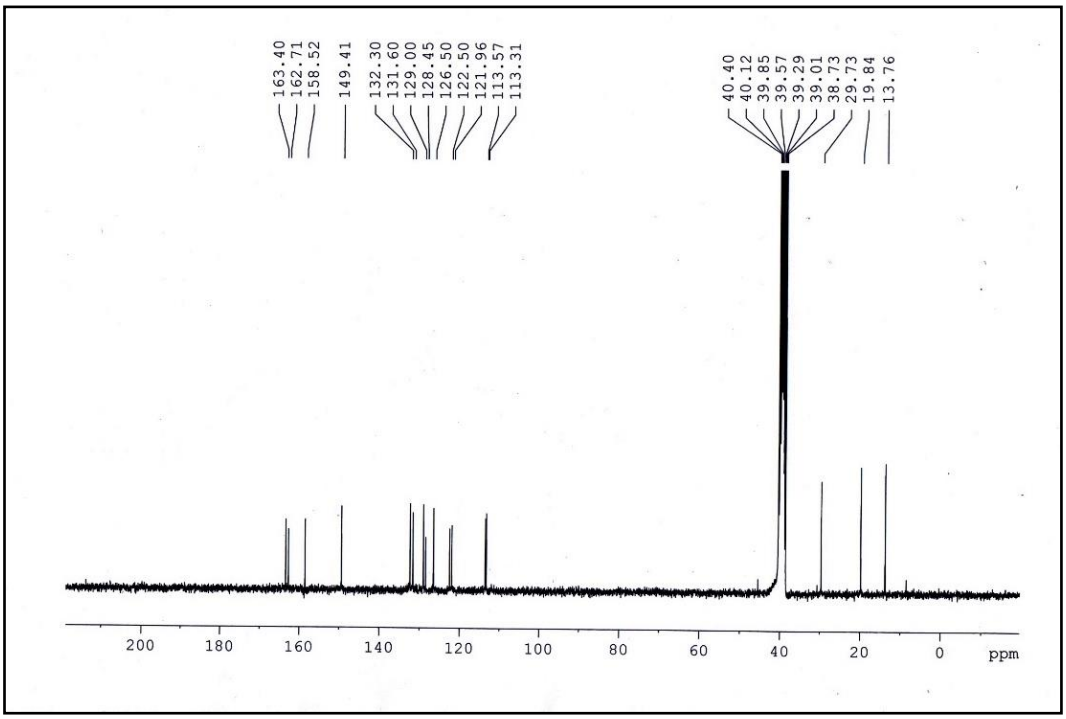

Figure S19: ^{13}C NMR of Compound **R1**

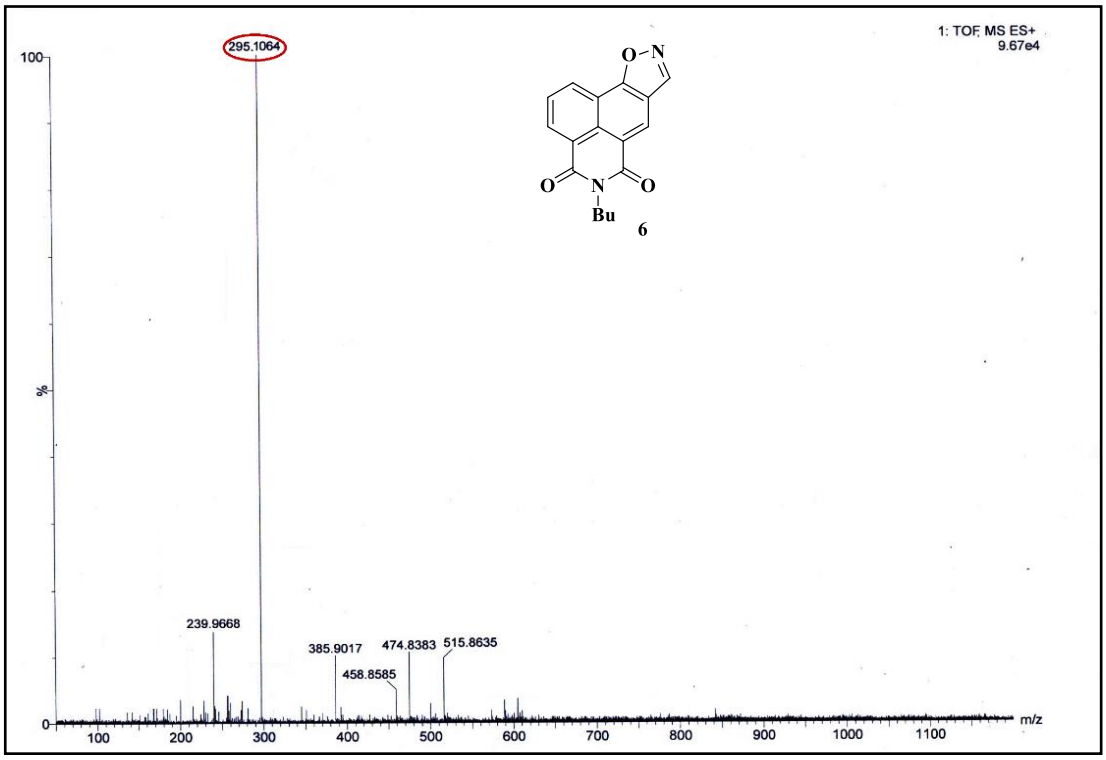

Figure S20: ESI-MS of Compound **6**

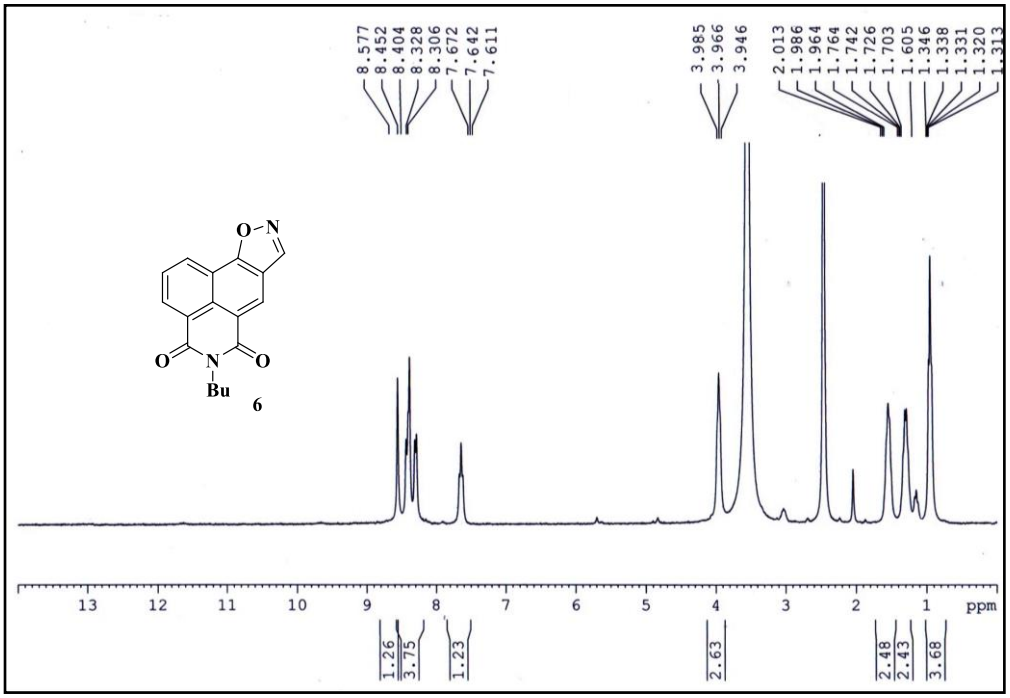

Figure S21: ^{1}H NMR of Compound **6**

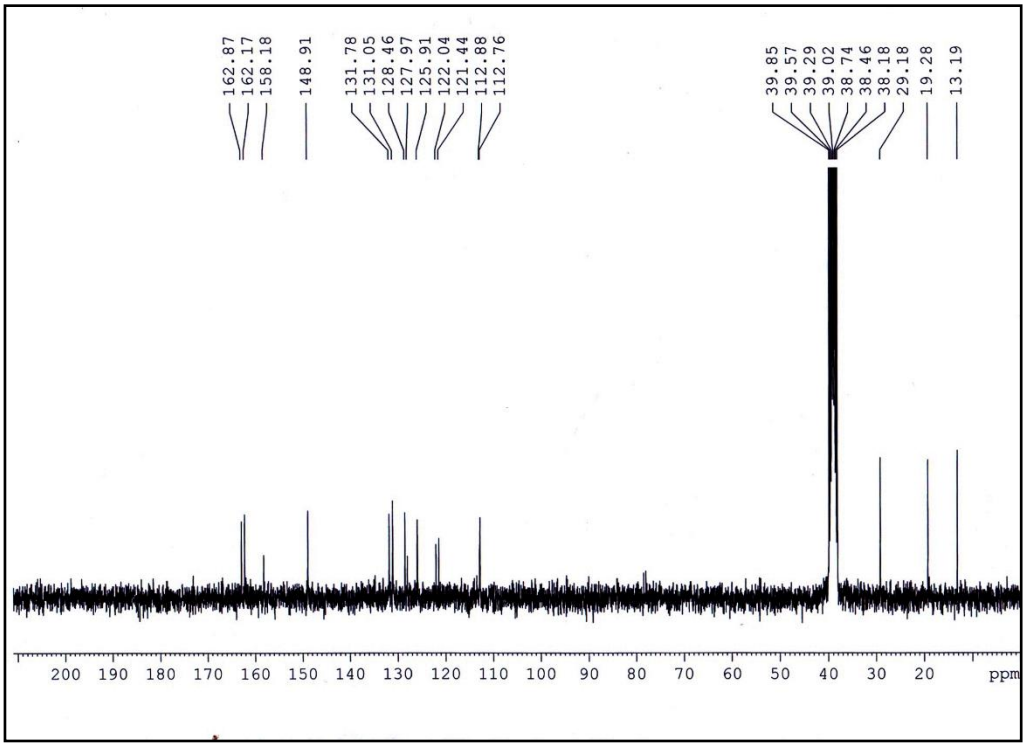

Figure S22: ^{13}C NMR of Compound **6**

12. Table S2: Competitive table of PCL/R1 nanofiber of different composition

PCL conc. (%) (Fixed 1% **R1**)	Diameter	Bead
20	300±40	yes
25	550±60	No
30	400±20	No (Smooth)

13. SEM images of R1/PCL composite fibers of different composition

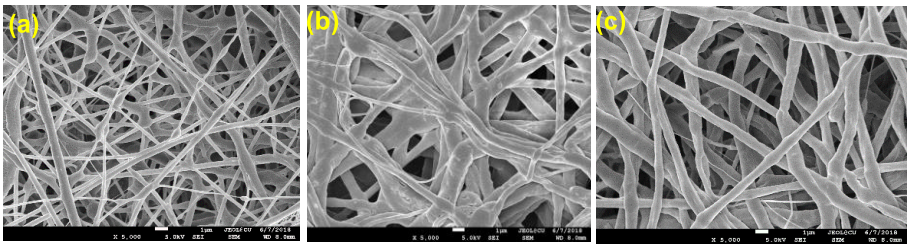

Figure S23: SEM image of PCL/**R1** nano fiber having (a)20%, (b) 25%, (c) 30% of PCL concentration to a fixed 1% of **R1** respectively.

14. SEM images of R1/PCL composite film in presence and absence of phosgene

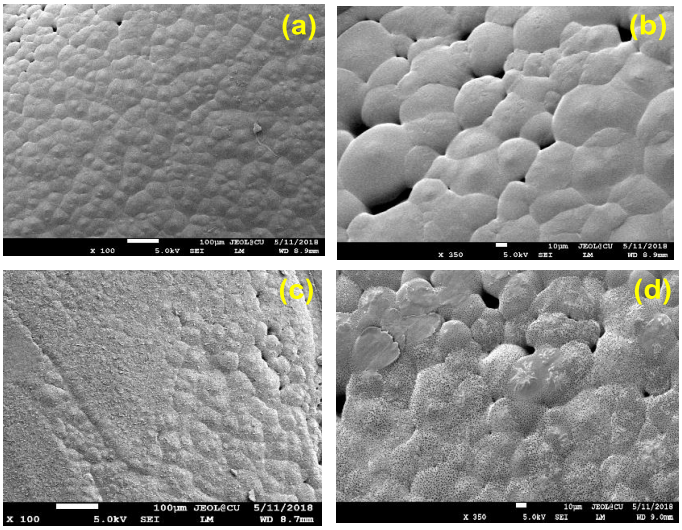

Figure S24: (a) SEM image of PCL/**R1** film, (b) that of higher magnification, (c) SEM image of PCL/**R1** film upon treatment with phosgene gas for 5 min., (d) that of higher magnification.

15. Change in color and fluorescence of different solid protocols in presence of phosgene

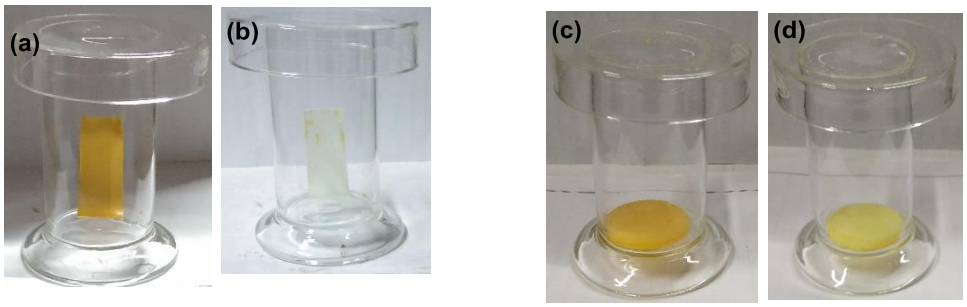

Figure S25: Naked eye color change of (a) **R1**/filter paper alone (b) upon treatment on phosgene atmosphere for 2 min. Naked eye color change of (c) **R1**/ PCL film (d) upon treatment on phosgene atmosphere for 2 min.

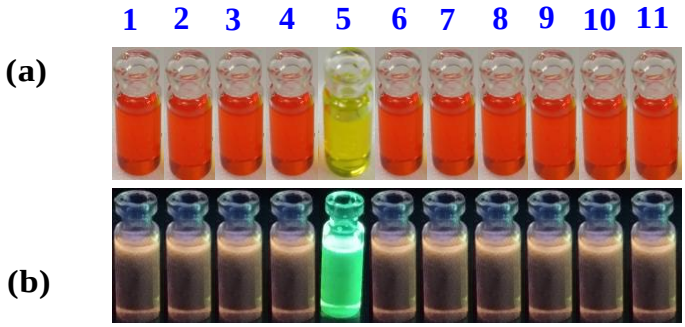

Figure S26: (a) Naked eye color change and (b) fluorescence change of **R1** (in ACCN) in presence of different analytes: 1. **R1**, 2. **R1**+ AcCl, 3. **R1**+ $SOCl_2$, 4. **R1**+TOsCl, 5. **R1**+ $COCl_2$, 6. **R1**+ SO_2Cl_2, 7. **R1**+ $(COCl)_2$, 8. **R1**+ DECP, 9. **R1**+ $POCl_3$, 10. **R1**+ HCHO, 11. **R1**+ NO.

16. Absorbance spectra of R1/PCL nanofiber in presence of phosgene in different time interval

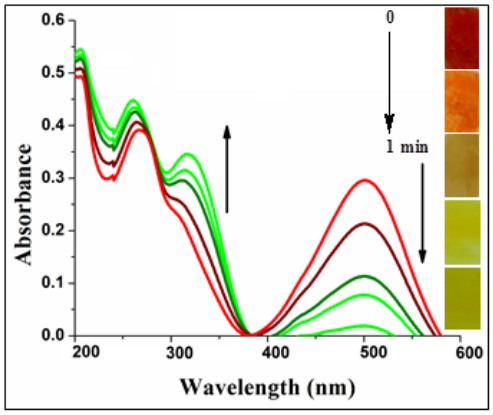

Figure S27: Absorbance spectra of PCL/**R1** nanofiber in phosgene atmosphere (0 to 1 min). Inset: Naked eye color change of PCL/**R1** nanofiber in phosgene atmosphere (0 to 1 min).

17. Table S3: **Competitive table of previously reported phosgene sensors with our sensor**

Compound	Ratiometric	LOD	Response time	Detection in polymer film and nano fiber	Selectivity	Ref.
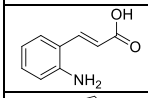	No	1 nm	-	No	yes	2
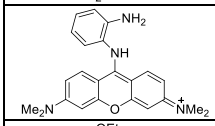	No	20 nM (triphosgene)	Several seconds	No	yes	3
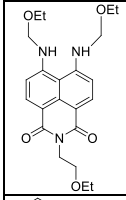	yes	1.3 nM (triphosgene) & (4 ppm gas)	20 min	No	yes	4
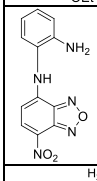	No	7 nM	150 s	Only nano fiber	yes	5
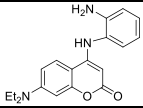	No	3 nM & 10 ppm gas	< 30 sec.	No	yes	6
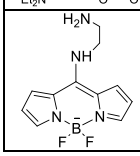	Yes	0.12 nM & (0.5 ppm gas)	1.5 sec.	No	yes	7

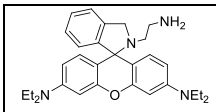	**No**	**50 nM (Triphosgene)& (0.8 ppm gas)**		**No**	**yes**	**8**
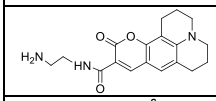	**No**	**5 µM**	**Within sec.**	**No**	**yes**	**9**
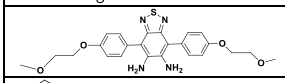	**No**	**20 nM**	**20 min**	**NO**	**NO**	**10**
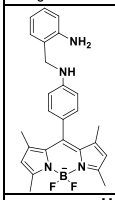	**No**	**179 nM & 10 ppm gas**	**< 10 sec.**	**NO**	**yes**	**11**
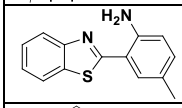	**yes**	**0.14 ppm**	**4 min**	**NO**	**yes**	**12**
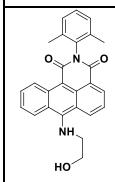	**yes**	**2.3 nM** **(20-90 ppm gas)**	**< 5 min**	**NO**	**yes**	**13**
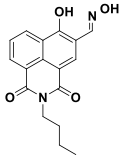	**yes**	**0.09 nM in solution and 0.087 ppm in gas phase**	**< 1.5 sec. in solution and < 5 sec. in solid phase**	**Yes**	**yes**	**This Work**

18. Table S4. Selected electronic excitation energies (eV), oscillator strengths (f), main configurations, and CI Coefficients of all the complexes. The data were calculated by TDDFT//B3LYP/6-31+G(*d,p*) based on the optimized ground state geometries

Molecules	Electronic Transition	Excitation Energy[a]	f[b]	Composition[c]	(composition) %
R1	$S_0 \rightarrow S_1$	**2.5077 eV 494.41 nm**	**0.7095**	**H → L**	**98.3**
Compound 6	$S_0 \rightarrow S_1$	**3.7810 eV 328.06 nm**	**0.6349**	**H → L**	**96.7**
	$S_0 \rightarrow S_2$	**4.8704 eV 254.58 nm**	**0.2541**	**H-1→ L**	**87.2**

[a] Only selected excited states were considered. The numbers in parentheses are the excitation energy in wavelength. [b] Oscillator strength. [c] H stands for HOMO and L stands for LUMO.

19. Table S5. Energies of the highest occupied molecular orbital (HOMO) and lowest unoccupied molecular orbital (LUMO)

Species	E_{HOMO} (a.u)	E_{LUMO}(a.u)	ΔE(a.u)	ΔE(eV)	ΔE(kcal/mol)
R1	-0.23416	-0.14202	0.09214	2.5077	57.8
Compound 6	-0.25091	-0.11025	0.14074	3.7792	87.1

20. HOMO-LUMO distribution of R1 and Compound 6

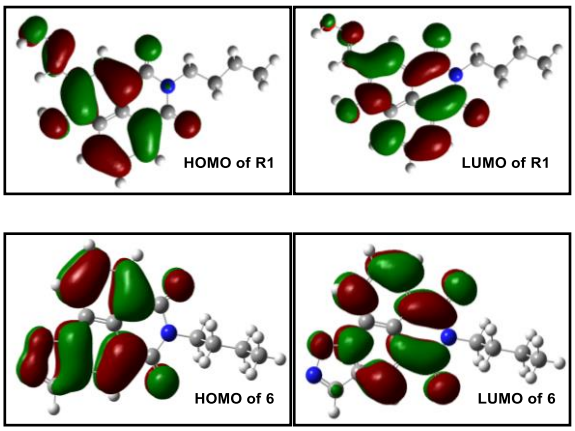

Figure S28: HOMO-LUMO distribution of **R1** and Compound 6.

21. ESIPT mode of R1

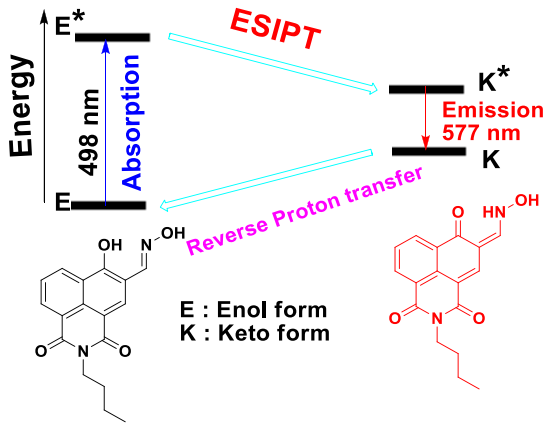

Scheme 3: ESIPT mode of **R1**

22. Table S4: Saturation limit of different compounds to phosgene

Compound	Saturation limit (ppm)
R1/PCL nanofiber	**0.24**
R1/PCL film	**0.33**
R1/filter paper	**0.38**

23. Temperature effect

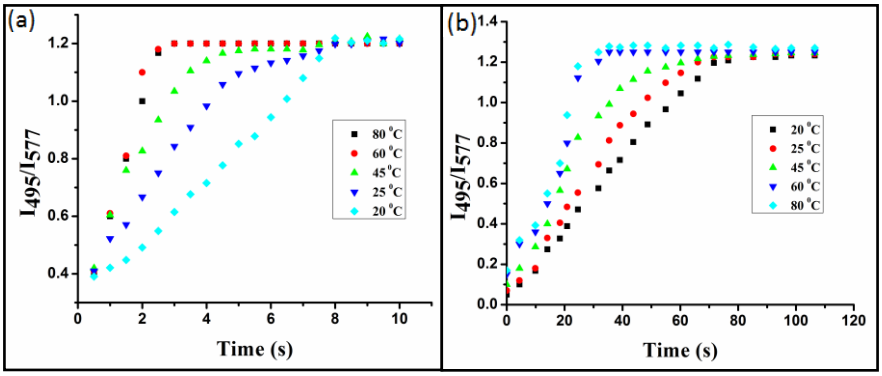

Figure S29: Temperature dependent fluorescence spectra (at different time interval) of (a) **R1**/PCL nano fiber and (b) **R1**/filter in presence of phosgene (0.5 ppm).

24. Humidity effect

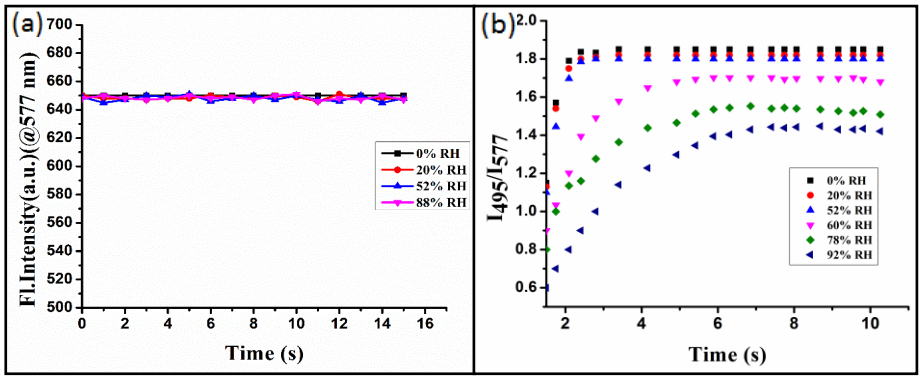

Figure S30: Relative humidity (RH) dependent fluorescence spectra (at different time interval) of (a) PCL nano fiber and (b) **R1**/PCL nano fiber in presence of phosgene (0.5 ppm).

25. Reusability test

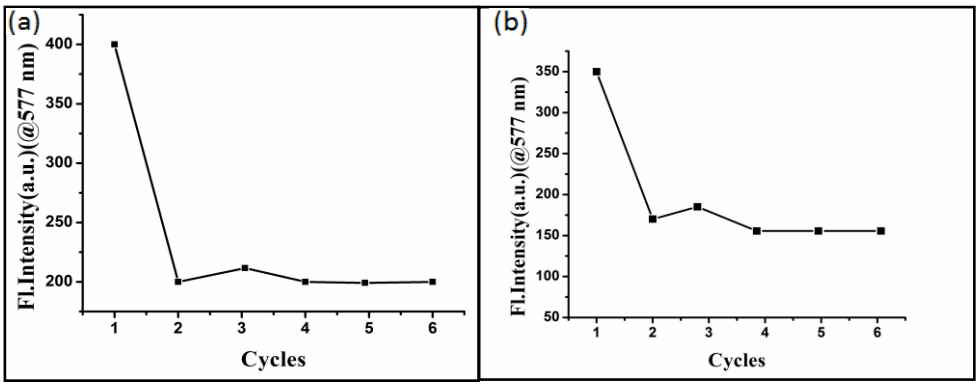

Figure S31: (a) Cycles of successive phosgene addition followed by heating of (a) **R1**/PCL nano fiber (for each 5 seconds) and (b) of **R1**/filter paper (for each 40 seconds.).

26. Photo stability

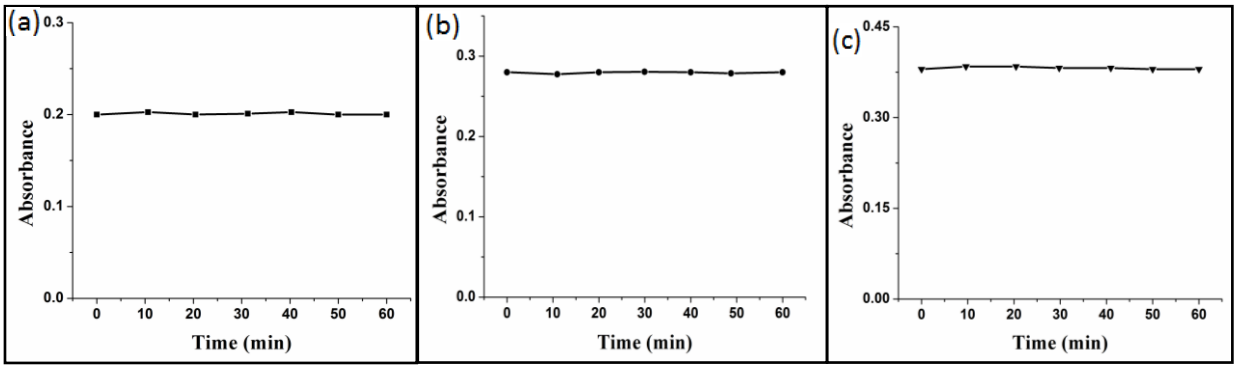

Figure S32: Time variation of (a) **R1**/ filter paper, (b) **R1**/PCL film and (c) **R1**/PCL nano fiber absorption peak at 498 nm after UV irradiation.

27. References

1) L. Song, Y. Yang, Q. Zhang, H. Tian, W. Zhu, *J. Phys. Chem. B.*, 2011, **115**, 14648–14658.

2) P. Kundu and K. C. Hwang, *Anal. Chem*., 2012, **84**, 4594−4597.

3) X. Zhou, Y. Zeng, C. Liyan, X. Wu, J. Yoon, *Angew. Chem., Int. Ed.*, 2016, **55**, 4729−4733.

4) S. L. Wang, L. Zhong and Q. H. Song, *Chem. Commun*., 2017, **53**, 1530-1533.

5) Y. Hu, L. Chen, H. Jung, Y. Zeng, S. Lee, K. M. K. Swamy, X. Zhou, M. H. Kim and J. Yoon, *ACS Appl. Mater. Interfaces*, 2016, **8**, 22246–22252.

6) H. C. Xia, X. H. Xu and Q. H. Song, *ACS Sens*., 2017, **2**, 178-182.

7) Y. Zhang, A. Peng, X. Jie, Y. Lv, X. Wang and Z. Tian, *ACS Appl. Mater. Interfaces*, 2017, **9**, 13920–13927

8) X. Wu, Z. Wu, Y. Yang, S. Han, *Chem. Commun*. 2012, **48**, 1895−1897.

9) Y. Zhang, X. Shao, Y. Wang, F. Pan, R. Kang, F. Peng, Z. Huang, W. Zhang, and W. Zhao, *Chem. Commun.*, 2015**, 51**, 4245-4248.

10) W. Q. Zhang, K. Cheng, X. Yang, Q. Y. Li, H. Zhang, Z. Ma, H. Lu, H. Wu and X. J. Wang, *Org. Chem. Fr ont*, 2017, **4**, 1719-1725

11) M. Sayar, E. Karakuş, T. Güner, B. Yildiz, U. H. Yildiz and M. Emrullahoğlu, *Chem. Eur. J.*, 2018, **24**, 3136-3140.

12) L. Chen, D. Wu, J. –M. Kim, and J. Yoon, *Anal. Chem*., 2017, **89**, 12596−12601.

13) Q. Hu, C. Duan, J. Wu, D. Su, L. Zeng and R. Sheng, *Anal. Chem*., 2018, **90**, 8686−8691.